

Long Gamma Ray Bursts Trace The Star Formation History

Shlomo Dado¹ and Arnon Dar¹

ABSTRACT

We show that if the broad-line supernova explosions of type Ic (SNeIc) produce the bulk of the observed long duration gamma ray bursts (LGRBs), which include both the high and low-luminosity LGRBs and the X-ray flashes (XRFs), and if LGRBs have the geometry assumed in the cannonball (CB) model of LGRBs, then their rate measured by Swift and their redshift distribution are consistent with the star formation rate (SFR) over the entire range of redshifts where the SFR has been measured with sufficient accuracy.

Subject headings: supernovae: general

1. Introduction

Core collapse supernovae are produced by the explosive death of short-lived massive stars. Although very bright in optical light, ordinary core collapse supernovae are not bright enough to be resolved in galaxies with redshift $z > 1$. As such, they can be used to trace the star formation history only up to redshifts $z \sim 1$.

Gamma-ray bursts (GRBs), the most luminous known electromagnetic events since the Big Bang, can be detected in MeV γ -rays up to very large redshifts, $z \gg 10$, with current instruments aboard satellites. Mounting photometric and spectroscopic evidence indicates that both long duration gamma ray bursts (LGRBs) and low luminosity X-ray flashes (XRFs) are produced by highly relativistic jets ejected in core collapse supernovae explosions of type Ic (SNeIc) of very massive stars at the end of their short life¹. This suggests that the cosmic rate of LGRBs may trace the cosmic star formation rate (Wijers et al. 1998) back to very large redshifts beyond those accessible to optical measurements. However, it has been claimed that the observed rate of LGRBs and XRFs follows neither the rate of SNeIc nor the

¹Physics Department, Technion, Haifa 32000, Israel

¹The only known exceptions, GRBs 060614 and 060505 (Fynbo et al. 2006; Della Valle et al. 2006; Gal-Yam et al. 2006) could have been produced in the death of massive stars, which generate very faint or failed supernovae (see, e.g., Dado et al. 2008).

star formation rate (SFR): Unlike the SFR (in a comoving unit volume) that first increases with redshift, the observed LGRB rate (LGRBR) in the range $z < 0.1$ first decreases with increasing redshift (e.g., Guetta & Della Valle 2007), while at larger redshifts it increases faster than the SFR (Daigne et al. 2006; Le & Dermer 2007; Yuksel et al. 2007; Salvaterra & Chincarini 2007; Li 2008; Kistler et al. 2008; Salvaterra et al. 2009). The discrepancy at small z was interpreted as evidence that low luminosity LGRBs and XRFs and ordinary LGRBs with much higher luminosity belong to physically distinct classes (Soderberg et al. 2004; Cobb et al. 2006; Liang et al. 2007; Soderberg et al. 2006, Pian et al. 2006, Amati et al. 2007, Chapman et al. 2007). The relative rate $\Psi(z)=\text{LGRBR}/\text{SFR}$ was claimed to behave like $\Psi(z) \propto (1+z)^\alpha$ with $\alpha \approx 0.5$ in the range where both are well observed (e.g., Robertson & Ellis 2012, Wei et al. 2013).

The photometric evidence (see, e.g., Dado et al. 2002, Zeh et al. 2004 and references therein) and spectroscopic evidence (see, e.g., Stanek et al. 2003, Hjorth et al. 2003, Wei et al. 2013, Cenko et al. 2013) that broad-line SNeIc produce both low luminosity XRFs and high luminosity LGRBs suggests that XRFs are ordinary LGRBs viewed far off-axis (Dado et al. 2004), and that perhaps the different behaviour of the LGRBR and SFR as function of redshift, both at very low and very high redshifts, is because of observational selection effects. Indeed, the inferred evidence of a different behaviour of the LGRBR than that of the SFR at both low and high redshifts involved the assumption that the beaming fraction $f_b = \langle (1 - \cos\theta_j) \rangle$ of detectable LGRBs is independent of z . This assumption is valid in the standard conical fireball (FB) models of GRBs because θ_j , the opening angle of the conical jet, which produces the observed GRB, is much larger than the relativistic beaming angle $\theta_b = 1/\gamma$ associated with the jet bulk motion Lorentz factor γ . Such a jet produces an afterglow with an achromatic temporal break at a time that is correlated to the prompt γ -ray emission properties, as well as closure relations between the temporal and spectral behaviours before the break and after the break (Rhoads 1997,1999, Sari et al. 1999). But, all these predictions turned out to be at odds with the observed properties of the afterglows of most LGRBs (see, e.g., Dado & Dar 2013 and references therein).

In the cannonball (CB) model of GRBs (Dar and De Rùjula 2004 and references therein), because of relativistic beaming, Doppler shift and time aberration, the energy-flux F from a highly relativistic cannonball (plasmoid) with bulk motion Lorentz factor $\gamma \gg 1$ and Doppler factor δ decreases very rapidly, like $F \propto \gamma^2 \delta^4 \rightarrow \theta^{-8}$, when the viewing angle θ relative to the CB's direction of motion satisfies $1/\gamma^2 \ll \theta^2 \ll 1$. This is because $\delta = [1/(\gamma(1 - \beta \cos\theta))] \approx 2\gamma/(1 + \gamma^2 \theta^2) \propto \theta^{-2}$ for $\theta^2 \ll 1$ and $\gamma^2 \theta^2 \gg 1$. As shown in section 3, because of this rapid decline of the γ -ray flux with viewing angle and the detector flux threshold, only a fraction $f_b(z) = 1 - \cos\theta_{\max} \propto [D_L(z)]^{-1/2}$ of GRBs at redshift z with a luminosity above the detector threshold can be detected. In this paper we show that such a decline in the

beaming fraction $f_b(z)$ of bi-polar LGRBs and the observed SFR that was compiled and standardized by Hopkins and Beacom (2006) and by Reddy and Steidel (2009), reproduce quite well the observed LGRBR without invoking a relative evolution.

2. The cosmic rate of LGRBs

In the CB model, LGRBs are produced in SNeIc by highly relativistic bipolar jets of plasmoids (CBs) ejected in accretion episodes of fall-back material on the newly formed compact object (e.g., Dar & De Rújula 2004 and references therein). Because of relativistic beaming, such LGRBs can be observed only from directions near the jet direction. In SNeIc that produce observable GRBs, the interaction of the highly relativistic jet with the sub-relativistic supernova ejecta results in much higher observed velocities of the ejecta towards the observer and consequently in absorption lines of the ejecta much broader than those usually observed during the photospheric phase of ordinary SNeIc that are not accompanied by an observable GRB. If most SNeIc produce GRBs that point away from Earth, as assumed in the CB model, then the observed cosmic rate of GRBs is the cosmic rate of SNeIc (SNIcR) multiplied by the beaming factor

$$\frac{d\dot{N}_{GRB}}{dz} \approx C f_b(z) SNIcR(0) \frac{SFR(z)}{SFR(0)} \frac{dV_c(z)}{dz} \frac{1}{1+z}, \quad (1)$$

where C is the fraction of the sky covered by the GRB detector and $dV_c(z)/dz$ is the comoving volume at redshift z . In a standard Λ CDM cosmology,

$$\frac{dV_c(z)}{dz} = \frac{c}{H_0} \frac{4\pi [D_c(z)]^2}{\sqrt{(1+z)^3 \Omega_M + \Omega_\Lambda}}, \quad (2)$$

where H_0 is the current Hubble constant, Ω_M and Ω_Λ are, respectively, the current density of ordinary energy and of dark energy, in critical energy-density units, and $D_c(z)$ is the comoving distance at redshift z , which satisfies

$$D_c(z) = \frac{c}{H_0} \int_0^z \frac{dz'}{\sqrt{(1+z')^3 \Omega_M + \Omega_\Lambda}}. \quad (3)$$

3. The beaming factor in the CB model

The CB model, its predictions and their extensive comparisons with GRB observations have been described in great detail in many publications (see, e.g., Dar and De Rújula 2004

for a review, Dado et al. 2009a,b for comparisons with observations). For readers unfamiliar yet with the CB model, a short description of the model is enclosed in Appendix I.

In the CB model, the Doppler shift, relativistic beaming and time aberration of the observed radiation yield strong dependence of the observed properties of GRBs on the bulk motion Lorentz and Doppler factors of the CBs (e.g., Dar and De Rújula 2000, 2004, Dado and Dar 2013 and references therein). In particular, the peak luminosity of LGRBs satisfies $L_p = L_0 \gamma^2 \delta^4$. Because of the detector energy-flux threshold F_{thr} , LGRBs at redshift z are detectable only when

$$L_p = L_0 \gamma^2 \delta^4 > 4 \pi [D_L(z)]^2 F_{thr}, \quad (4)$$

where $D_L(z) = (1 + z) D_c$ is the luminosity distance to redshift z . Fig. 1 presents the distribution of $L_p(z)$ of Swift LGRBs as a function of redshift for all Swift LGRBs, which were detected before November 15, 2013 and are listed in the Greiner catalog of GRBs (<http://www.mpe.mpg.de/~jcg/grbgen.html>) and whose L_p was measured by Konus-Wind or Fermi GBM and reported in the GCN archive (Barthelmy 1997). Also shown by lines are the lower limit behaviour expected from Eq. (4) and the upper limit $max L_p(z) = const$ for LGRB population with no redshift evolution.

But, $1 - \cos\theta \approx 1/(\gamma \delta)$ for $\gamma^2 \theta^2 \gg 1$. Consequently, Eq. (4) implies that LGRBs at redshift z are detectable only if their viewing angle satisfies $(1 - \cos\theta) \leq (1 - \cos\theta_{max}) = [L_0/4 \pi \gamma^2 [D_L(z)]^2 F_{thr}]^{1/4} \propto [D_L(z)]^{-1/2}$, which yields a beaming fraction that depends on redshift,

$$f_b(z) = (1 - \cos\theta_{max}) \propto [D_L(z)]^{-1/2}. \quad (5)$$

In the CB model, the lower limit on the Doppler factor of LGRBs $min \delta(z) \propto [D_L(z)]^{1/2}$ that follows from Eq. (4) and yields Eq. (5), also yields bounds on many other observed properties of LGRBs as function of redshift, which provide independent additional tests of the redshift dependence of the beaming fraction as given by Eq. (5). For instance, in the CB model, the equivalent isotropic γ -ray luminosity, the peak γ -ray energy, and the break-time of the X-ray afterglow in the GRB rest frame satisfy, respectively, $E_{iso} \propto \gamma \delta^3$, $E'_p \propto \gamma \delta$ and $t'_b \propto 1/\gamma \delta^2$ (e.g., Dar and De Rújula 2000, 2004, Dado and Dar 2012, and references therein). These CB model relations lead to correlations among these observables which were predicted long before they were discovered empirically. They also yield the CB model predictions, $min E_{iso}(z) \propto [D_L(z)]^{3/2}$, $min E'_p(z) \propto [D_L(z)]^{1/2}$ and $max t'_b(z) \propto [D_L(z)]^{-1}$, which are shown in Figs. 2-4 for the Swift LGRBs with known redshift that were detected before November 15, 2013 and are listed in the Greiner's catalog of GRBs. Any one of these limits can be used to extract $f_b(z)$ from the observations displayed in Figs. 1-4.

The normalization of $f_b(z)$, however, can be obtained most simply from the CB model

relation $E'_p \approx \gamma \delta \epsilon_g$ (e.g., Dar and De Rújula 2004), where E'_p is the peak energy of the prompt gamma rays of LGRB in its rest frame (indicated by a prime), which are produced by inverse Compton scattering of glory photons - a light halo with a bremsstrahlung energy spectrum $\epsilon dn_\gamma/d\epsilon \propto \exp(-\epsilon/\epsilon_g)$ surrounding the progenitor (a Wolf-Rayet star) that was formed by scattered stellar light from the pre-supernova ejecta blown from the star in eruptions sometime before its SNIc explosion: If z_m is the redshift of the LGRB with the lowest measured E'_p ,

$$f_b(z) \approx \frac{\epsilon_g}{\min E'_p} \left[\frac{D_L(z_m)}{D_L(z)} \right]^{1/2}. \quad (6)$$

For a typical glory of Wolf-Rayet stars, $\epsilon_g \sim 3$ eV corresponding to a surface temperature of $\sim 35,000$ K. XRF060218 (Campana et al. 2006) at redshift $z = 0.0331$ (Mirabal and Halpern 2006) had $E'_p = 4.5$ keV the lowest E'_p value measured for a Swift GRB. In terms of these values, Eq. (5) can be written as

$$f_b(z) = 1 - \cos\theta_{max} \approx 6.6 \times 10^{-4} \left[\frac{D_L(z)}{D_L(0.0331)} \right]^{-1/2}. \quad (7)$$

This beaming factor is shown in Fig. 5 as an upper bound line to the z -distribution of the $1 - \cos\theta$ values extracted from the CB model relation $1 - \cos\theta \approx 1/(\gamma \delta) = \epsilon_g/E'_p$ for the 134 Swift LGRBs and XRFs that were detected before November 15, 2013, have a known redshift listed in the Greiner catalog of GRBs and an E'_p value measured with Konus-Wind and/or with Fermi-GBM and reported in the archive of GCN circulars (Barthelmy 1997).

Note that for $z < 0.1$, where $D_L(z) \approx D_c(z) \approx cz/H_0$, Eq. (1) can be integrated analytically over time and redshift to yield the approximate behaviour,

$$N(< z) \approx C \text{ SNIc}R(0) T \frac{\epsilon_g}{\min E'_p} \frac{8\pi}{5} \left(\frac{c}{H_0} \right)^3 z_m^{1/2} z^{5/2}, \quad (8)$$

where T is the total observation time.

4. Comparison With Observations

Priors: In order to compare theory and observations, we have adopted:

- (a) The current best values of the cosmological parameters from the Planck data (Ade et al. 2013): a Hubble constant $H_0 = 67.3$ km/s Mpc $^{-1}$, $\Omega_M = 0.315$ and $\Omega_\Lambda = 0.685$.
- (b) The local rate 0.065 ± 0.032 SNU of SNIc estimated by Arbutina (2007), where SNU=SNU per $10^{10} L_\odot$ per century for the above value of H_0 . For a local luminosity density of $1.4 \times 10^8 L_\odot$ Mpc $^{-3}$, it yields $\text{SNIc}R(0) \approx (9.0 \pm 4.5) \times 10^{-6}$ Mpc $^{-3}$ y $^{-1}$.

(c) The star formation rate that was compiled and standardized by Hopkins and Beacom (2006) and by Reddy and Steidel (2009) from optical measurements. This standardized SFR is well approximated by a log-normal distribution,

$$\text{SFR}(z) \approx 0.25 e^{-[\ln((1+z)/3.16)]^2/0.524} \text{ M}_\odot \text{ Mpc}^{-3} \text{ y}^{-1}. \quad (9)$$

(d) The probability $\langle P(z) \rangle \approx 262/749 = 0.35$ of a Swift LGRB to have a measured redshift (from emission lines of the LGRB host galaxy and from absorption lines or photometry of its optical afterglow): Out of the 749 Swift LGRBs detected up to November 15, 2013, only about 50% have a detected optical afterglow, despite rapid optical follow up, and only 262 have a measured redshift. Probably, most of the "missing redshifts" are due to dust extinction, the limiting sensitivity of the telescopes, and the time it takes to acquire spectroscopic/photometric redshifts (e.g., Coward et al. 2012). From the relative number of LGRB redshift measurements by the three methods as function of z reported in GCN catalog (Barthelmy 1997), we have estimated that $P(z) \approx 0.684 e^{-z/0.5} + 0.316$. However, the use of this rough estimate instead of $P(z) = \langle P(z) \rangle$ has a negligible effect on our results, except for $z \lesssim 0.1$ (see below).

Tests of the SFR-LGRBR connection: Because of the different sensitivities and sky coverage of different GRB missions, we have limited our comparison to the 262 LGRBs and XRFs with known z that were detected by Swift before November 15, 2013 and are listed in the Greiner catalog of GRBs. For this choice:

The daily rate of LGRBs obtained by integrating Eq. (1) over redshift, using Eqs. (2),(3),(7) and the priors (a)-(c), is $\text{LGRBR} \approx 2.1 \pm 1.5 \text{ day}^{-1}$ of observable LGRBs (high luminosity GRBs + low luminosity GRBs + XRFs) for a full sky coverage ($C = 1$). The 749 LGRBs detected by Swift before November 15, 2013 with a sky coverage of $C \approx 1.4/4\pi = 0.11$ (Salvaterra & Chincarini 2007), yield $\approx 2.07 \text{ day}^{-1}$ Swift-like LGRBs over the entire sky, in agreement with that obtained from Eq. (1).

The redshift distribution of Swift LGRBs with known redshift is compared in Fig.6 to that predicted by Eqs. (1)-(3),(7) with the priors (a)-(d). The predicted mean redshift, $\langle z \rangle = 2.08$, is consistent with $\langle z \rangle = 2.12$ obtained from the reported redshifts of the 262 Swift LGRBs with known redshift, which are listed in the Greiner GRB catalog. The agreement between the expected and the observed distribution is quite good ($\chi^2/df = 25.5/26 = 0.98$, significance level 49%, assuming Poisson statistics, i.e., $\sigma_i = \sqrt{N_i}$ where N_i is the observed number of LGRBs in bin i). The bins 21-30 and 31-50 were converted to two bins $5 < z \leq 7$ and $7 < z \leq 10$, respectively, in order to have $N_i \geq 5$. Similar agreement ($\chi^2/df = 48.88/49 = 1.00$, significance level 48%) was obtained when all the 50 z bins of width $\Delta z = 0.2$ shown in Fig. 6 were included in the χ^2/df calculation but the standard

deviation errors $\sigma_i = \sqrt{N_i}$ were estimated from the predicted value of N_i . Similar agreement ($\chi^2/df = 7.56/7 = 1.08$, with a significance level of 37%, and $\chi^2/df = 5.02/5 = 1.00$ with a significance level of 41%, respectively) were obtained for the TOUGH (56 Swift LGRBs, Hjorth et al. 2012) and BAT6 (52 Swift LGRBs, Salvaterra et al. 2012) samples when they were compared with the CB model predicted distribution.

Fig. 6, however, indicates ~ 8 LGRBs deficiency of Swift LGRBs with measured redshift in the bin $1.8 \leq z \leq 2.0$, in the so called 'GRB redshift desert', which is believed to be due to an observational bias rather than a real deficiency (Coward et al. 2012). Indeed, the TOUGH, and in particular the BAT6 sample of bright Swift LGRBs (Salvaterra et al. 2012), have a redshift distribution where the 'GRB desert' is almost completely filled. Adding eight 'missing LGRBs' to the $[1.8 < z < 2.0]$ bin of the Swift distribution of 262 LGRBs improves the good agreement reported above to a remarkable agreement between the differential distribution predicted by the CB model and the observed distribution ($\chi^2/df = 15.8/24 = 0.66$, significance level 90%).

The cumulative distributions $N(< z)$ of the 262 and 270 (262+8 missing) Swift LGRBs with known redshift, which were detected before November 15, 2013, and the cumulative distributions predicted by the CB model (using Eqs. (1)-(3),(7) with the priors (a)-(d)) are compared in Figs. 7 and 8, respectively. Also shown in Figure 8 are the expected distribution in the standard fireball model with an assumed z -evolution of the LGRBR relative to the SFR of the form $LGRBR/SFR \propto (1+z)^\alpha$ with $\alpha = 0$ (no evolution) or $\alpha = 1/2$ (a best fit obtained by Robertson and Ellis (2012) and by Wei et al. (2013) to their selected samples of 112 and 86 bright Swift LGRBs, respectively, in the range $z \leq 4$). As can be seen by simple inspection of Figs. 7 and 8, the agreement between the observed and the CB model distributions of the complete sample of Swift LGRBs with known redshift ($0.0331 \leq z \leq 9.2$), is very good and becomes remarkable once the 'eight missing GRBs' are added to the $[1.8 < z < 2.0]$ bin².

The cumulative distribution shown in Fig. 8 allows alternative formal tests of goodness of fit, such as the Kolmogorov-Smirnov (KS) and Anderson-Darling (AD) statistical tests. Such tests also yield very high significance levels for the agreement between the observed CDF and the CB model CDF and rejection of the FB model CDFs with $\alpha \geq 0$ relative evolution. E.g., the KS statistic of the CB model fit, $D_{max}=0.0436$ for $n=262$ yields a significance level $> 90\%$, while models with $f_b = const$ with $\alpha=0, 0.5$ and 1.5 yield $D_{max}=0.151, 0.222$, and

² The sum of independent variables with a Poisson distribution is also a Poisson distribution with a mean and a variance equal to the sum of means and variances of the independent variables. Hence the standard deviation error of $N(< z)$ is $\sqrt{N(< z)}$. Moreover, the significance level of a χ^2 goodness of fit to the binned differential distribution is also the significance level of agreement between the corresponding binned theoretical and measured cumulative distribution functions (CDFs).

0.382, respectively with a significance level $\ll 1\%$.

The observed rate of low-luminosity LGRBs and XRFs was compared in Fig. 9 with that predicted by Eq. (7), assuming that the probability of obtaining the redshift of the host galaxies of very nearby LGRBs is $P(z) \approx 1$ rather than the mean value $P(z) \approx 0.35$ for the entire $0 \leq z \leq 10$ range. Also, because of the limited statistics, the true $f_b(z)$ for Swift LGRBs may lie somewhat above the upper limit shown in Fig. 5. Indeed, the lowest reported E'_p value of LGRB was $E'_p = 3.37 \pm 1.79$ keV for XRF020903 at $z = 0.25$ measured with the HETE satellite (Amati et al. 2002). With f_b estimated from these values and $P(z) = 1$, Eq. (6) yields 0.33, 1.4, 3, and 3.9 expected detections ($\pm 70\%$ estimated error) of LGRBs+XRFs with redshift smaller than 0.0331, 0.059, 0.080, and 0.089, respectively, which are the redshifts of XRF060218 (Mirabal and Halpern 2006), GRB100316D (Vergani et al. 2010), XRF051109B (Perley et al. 2006), GRB060505 (Ofek et al. 2007), the lowest z LGRBs that were detected by Swift during $T \approx 9$ years of observations (see the Greiner GRB catalog, <http://www.mpe.mpg.de/~jcg/grbgen.html>). The above predicted values are in agreement with the corresponding values 0, 1, 2, and 3 of the observed cumulative distribution. Moreover, since the launch of the BeppoSAX in 1996 only one GRB (980425 at $z = 0.0085$) was detected by the γ -ray satellites at a redshift smaller than 0.0331 during a combined effective observation time of roughly $T \approx 17$ Swift observation years, compared to 0.66 ± 0.46 expected in the CB model.

5. Discussion and conclusions

Star formation at redshifts $z > 6$ may have made an important contribution to the reionization of the universe, to its optical depth to the cosmic background radiations and to its metallicity at high redshifts. However, direct measurements of the star formation rate at redshifts $z \gtrsim 6$ and their correct interpretation are quite challenging (for a review, see, e.g., Robertson et al. 2010). Long duration GRBs, which are produced in SNeIc explosions of massive stars, and whose optical afterglows are visible at redshifts, which exceed by far those where direct measurements of the SFR are still possible, offer the possibility to extend the SFR 'measurements' to redshifts far beyond those of the direct measurements.

The measured rate of LGRBs as a function of redshift, however, was claimed to differ significantly from the observed SFR, both at low and high redshifts. The discrepancy at low redshift (approximately a factor ~ 100) was explained by assuming that LGRBs with low isotropic luminosities belong to a class different from that of LGRBs with high isotropic equivalent luminosities, which is at odds with the observations that both the low-luminosity and the high-luminosity LGRBs are produced by similar broad-line SNeIc. Moreover, the

assumption does not explain why the observed rate as function of redshift of low-luminosity LGRBs, which are produced by SNeIc, does not follow that of the SFR at $0 < z < 0.1$.

In the range $0.1 \leq z \leq 4$, the LGRBR was claimed to have a more rapid evolution relative to the SFR, which can be well parametrized by $(1+z)^{0.5}$. But, such a relative evolution (assuming a z -independent beaming factor), which was shown to fit well selected samples of bright Swift LGRBs with a known redshift in the range $z < 4$ (Robertson & Ellis 2012, Wei et al. 2013) fails to describe the complete distribution of Swift LGRBs with known redshift, which currently extends over $0.0331 \leq z \leq 9.2$. In fact, FB models with z -independent beaming factor and $\alpha \geq 0$ overpredict the high z SFR inferred from the abundance of UV-selected galaxies (Robertson & Ellis 2012 and references therein).

In this paper, however, we have shown that the above discrepancies may have been the result of assuming a redshift-independent beaming factor of LGRBs, which was adopted from the underlying current geometry of the standard conical fireball model of LGRBs. Once the assumed conical geometry of LGRBs is replaced by the geometry adopted in the cannonball model of GRBs, the beaming factor of LGRBs becomes z -dependent as a result of the detection threshold of GRBs. We have shown that this plus the assumption that all SNeIc produce LGRBs, most of which are beamed away from Earth, yields a theoretical rate of LGRBs, which correctly reproduces: (i) the full sky rate of cosmic LGRBs ($\approx 2.1 \text{ day}^{-1}$) above the Swift detection threshold, (ii) the observed distribution of Swift LGRBs with known redshift as a function of the redshift, and consequently (iii) the observed mean redshift $\langle z \rangle \approx 2.12$ of Swift LGRBs with known z , and (iv) the cumulative distribution $N(< z)$ of Swift LGRBs as a function of z between their lowest and highest observed redshifts.

We conclude that LGRBs seem to trace the SFR as a function of redshift at least up to $z \approx 6$, that probably most SNeIc produce LGRBs beamed away from Earth, and that the high-luminosity LGRBs and the low-luminosity LGRBs and XRFs seem to belong to the same class of SNIc-GRBs while the observed differences between them are produced by the strong dependence of the observed LGRB properties on detector threshold and on their Lorentz factor and viewing angle, which are well described by the cannonball model of GRBs.

6. Appendix I - Outline of the CB model of LGRBs

In the cannonball (CB) model of GRBs (Dado et al. 2002; Dar and De Rújula 2004; Dado et al. 2009a,b), LGRBs and their afterglows are produced by the interaction of bipolar jets of highly relativistic ($\gamma \gg 1$) plasmoids (CBs) of ordinary matter with the radiation and matter along their trajectory (Shaviv and Dar 1995, Dar 1998). Such jetted CBs are

presumably ejected in accretion episodes on the newly formed compact stellar object in core-collapse supernova (SN) explosions (Dar et al. 1992, Dar and Plaga 1999, Dar and De Rújula 2000). It is hypothesized that an accretion disk or a torus is produced around the newly formed compact object, either by stellar material originally close to the surface of the imploding core and left behind by the explosion-generating outgoing shock, or by more distant stellar matter falling back after its passage (Dar and De Rújula 2000, 2004). As observed in microquasars, each time part of the accretion disk falls abruptly onto the compact object, two CBs made of ordinary-matter plasma are emitted in opposite directions along the rotation axis from where matter has already fallen back onto the compact object due to lack of rotational support. The prompt γ -ray pulses and early-time X-ray flares are dominated by inverse Compton scattering (ICS) of glory photons - a light halo surrounding the progenitor star that was formed by stellar light scattered from the pre-supernova ejecta/wind blown from the progenitor star - by the CBs electrons. The ICS is overtaken by synchrotron radiation (SR) when the CB enters the pre-supernova wind/ejecta of the progenitor star.

Acknowledgement: We thank an anonymous referee for useful comments and suggestions.

REFERENCES

- Ade, P. A. R., et al. 2013, arXiv:1303.5076
- Amati, L., et al. 2002, *A&A*, 390, 81
- Amati, L., et al. 2007, *A&A*, 463, 913
- Arbutina, B., 2007, *Bulgarian J. of Phys. Supplement*, 34(s2), 271
- Barthelmy, S., 1997, http://gcn.gsfc.nasa.gov/gcn_main.html
- Campana, S., et al. 2006, *Nature*, 442, 1008
- Chapman R., et al. 2007, *MNRAS*, 382, L21
- Cenko, S. B., et al. 2013, *GCN Circ.* 14998
- Cobb, B. E., et al. 2006, *ApJ*, 645, L113
- Coward, D., et al. 2012, arXiv:1210.2488
- Dado, S. & Dar, A., 2012, *ApJ*, 749, 100
- Dado, S. & Dar, A., 2013, *A&A*, 558, A115

- Dado, S., Dar, A., & De Rújula, A., 2002, *A&A* 388, 1079
- Dado, S., Dar, A., & De Rújula, A., 2004, *A&A* 422, 381
- Dado, S., Dar, A., & De Rújula, A., 2008, *ApJ*, 2008, 678, 353
- Dado, S., Dar, A. & De Rújula, A. 2009a, *ApJ*, 696, 994
- Dado, S., Dar A. & De Rújula A., 2009b, *ApJ*, 693, 311
- Daigne, F., Rossi E. M., Mochkovitch R. 2006, *MNRAS*, 372, 1034
- Dar, A., 1998, *ApJ*, 500, L93
- Dar, A., et al. 1992, *ApJ*, 388, 164
- Dar, A. & De Rújula, A., 2000, arXiv:astro-ph/0008474
- Dar, A. & De Rújula, A., 2004, *Phys. Rept.* 405, 203
- Dar, A. & Plaga, R., 1999, *A&A*, 349, 259
- Della Valle, M., et al. 2006, *Nature*, 444, 1050
- Fynbo, J. P. U., et al. 2006, *Nature*, 444, 1047
- Gal-Yam, A., et al. 2006, *Nature*, 444, 1053
- Guetta, D. & Della Valle, M., 2007, *ApJ*, 657, L73
- Hjorth, J., et al. 2003, *Nature*, 423, 847
- Hjorth, J., et al. 2012, *ApJ*, 756, 187
- Hopkins, A. M. & Beacom J. F., 2006, *ApJ*, 651, 142
- Kistler, M. D., et al. 2008, *ApJ*, 673, L119
- Le, T. & Dermer C. D., 2007, *ApJ*, 661, 394
- Li, L.-X., et al. 2008, *MNRAS*, 388, 1487
- Liang, E., et al. 2007, *ApJ*, 662, 1111
- Mirabal, N. & Halpern, J. P. 2006, *GCN Circ.* 4792
- Ofek, E. O., et al. 2007, *ApJ* 662, 1129

- Perley, D. A., et al. 2006, GCN Circ. 5387
- Pian, E., et al. 2006, Nature, 442, 1011
- Reddy, N. A. & Steidel, C. C., 2009, ApJ, 692, 778
- Rhoads, J. E., 1997, ApJ, 487, L1
- Rhoads, J. E., 1999, ApJ, 525, 737
- Robertson, B. E., et al. 2010, Nature, 468, 49
- Robertson, B. E. & Ellis R. S., 2012, ApJ, 744, 95
- Sari, R., Piran, T., & Halpern, J. P., 1999, ApJ, 519, L17
- Salvaterra, R. & Chincarini, G., 2007, ApJ, 656, L49
- Salvaterra, R., et al. 2009, MNRAS, 396, 299
- Salvaterra, R., et al. 2012, ApJ, 749, 68
- Shaviv, N. J. & Dar, A., 1995, ApJ, 447, 863
- Soderberg, A. M., et al. 2004, Nature, 430, 648
- Soderberg, A., et al. 2006, Nature, 442, 1014.
- Stanek, K. Z., et al. 2003, ApJ, 591, L17
- Vergani, S. D., et al 2010, GCN Circ. 10512
- Wei, J., et al. 2013, arXiv:1306.4415
- Wijers, R. A. M., et al. 1998, MNRAS, 294, L13
- Yuksel, H., Kistler, M. D., 2007, PhRvD, 75, 083004
- Zeh, A., Klose, S. & Hartmann, D. H., 2004, ApJ, 609, 952

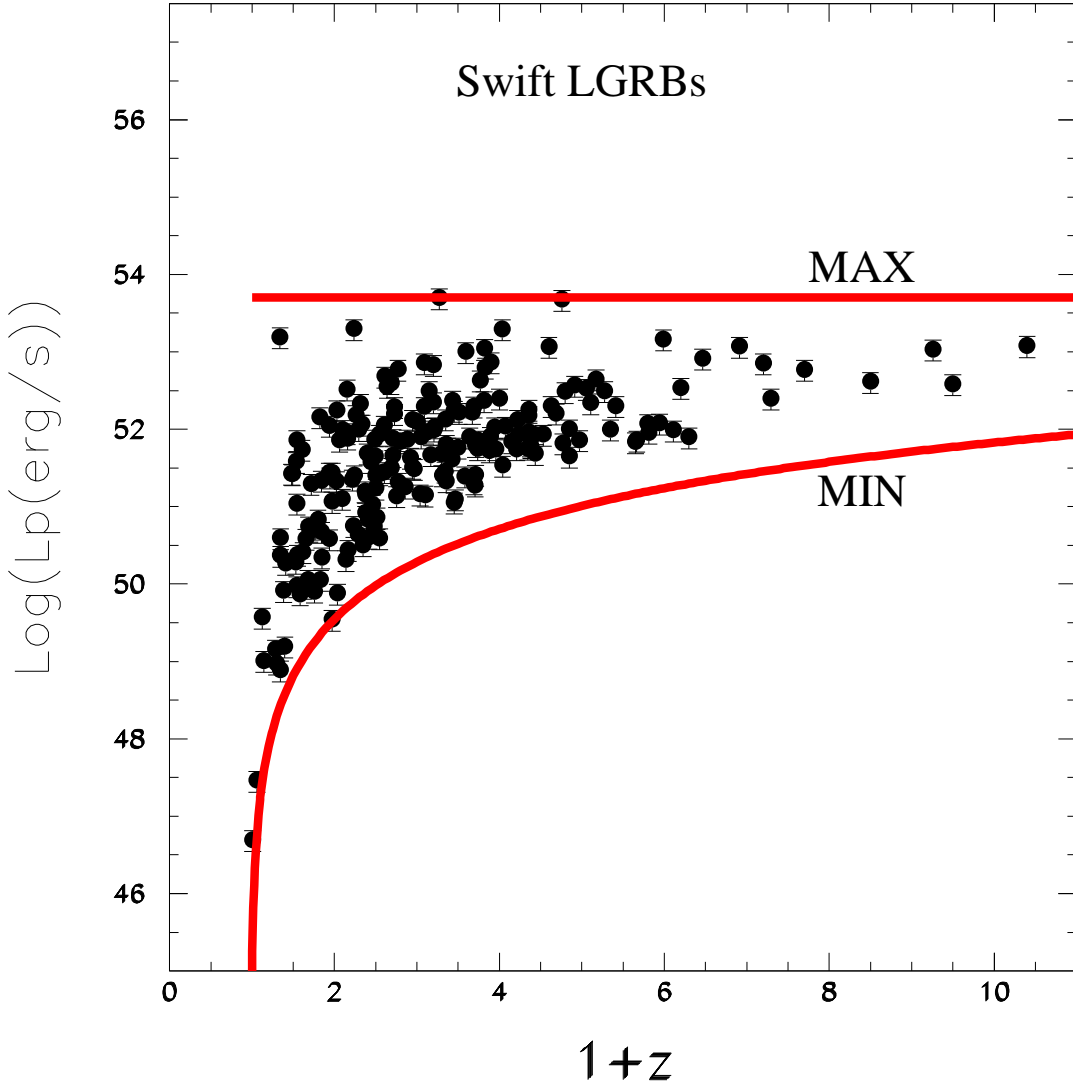


Fig. 1.— The distribution of the isotropic equivalent peak gamma-ray luminosity $L_p(z)$ as function of redshift of Swift LGRBs which were detected before November 15, 2013 and are listed in the Greiner catalog of GRBs, and whose L_p was measured With Konus-Wind and/or Fermi GBM and reported in the GCN archive (Barthelmy 1997). Also shown are the best fit lower limit line $min L_p(z) \propto [D_L(z)]^2$ and the upper limit line $max L_p = const$ line expected in the CB model of LGRBs.

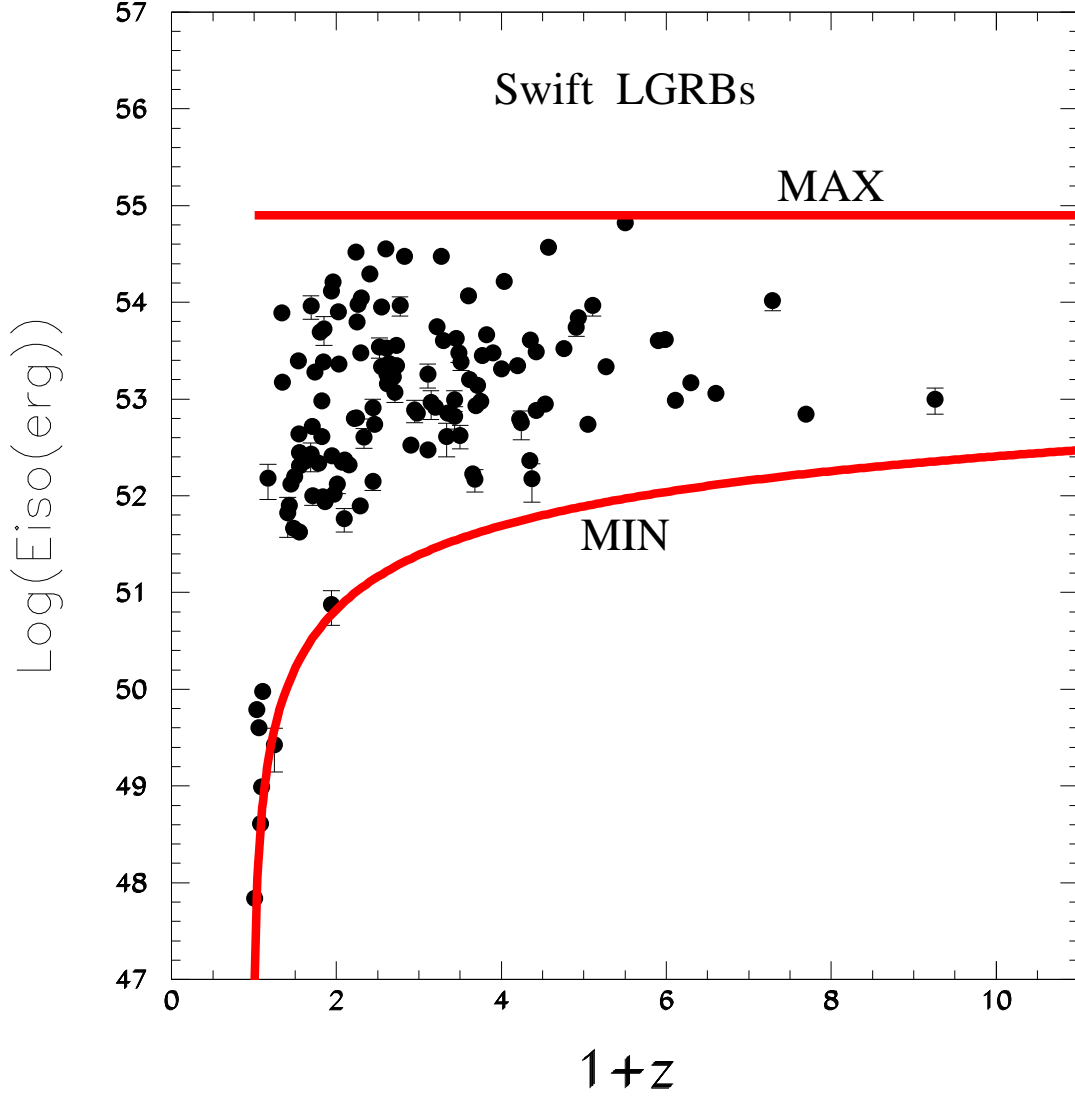


Fig. 2.— The distribution of the isotropic equivalent γ -ray energy E_{iso} as a function of redshift for all LGRBs which were detected by Swift before November 15, 2013 and are listed in the Greiner catalog of GRBs, and whose redshift and E_{iso} were measured. Also shown are the CB model best fit lower and upper limit lines, $min E_{iso}(z) \propto [D_L(z)]^{3/2}$, and $max E_{iso}(z) = const$, respectively, of the measured E_{iso} distribution as function of z .

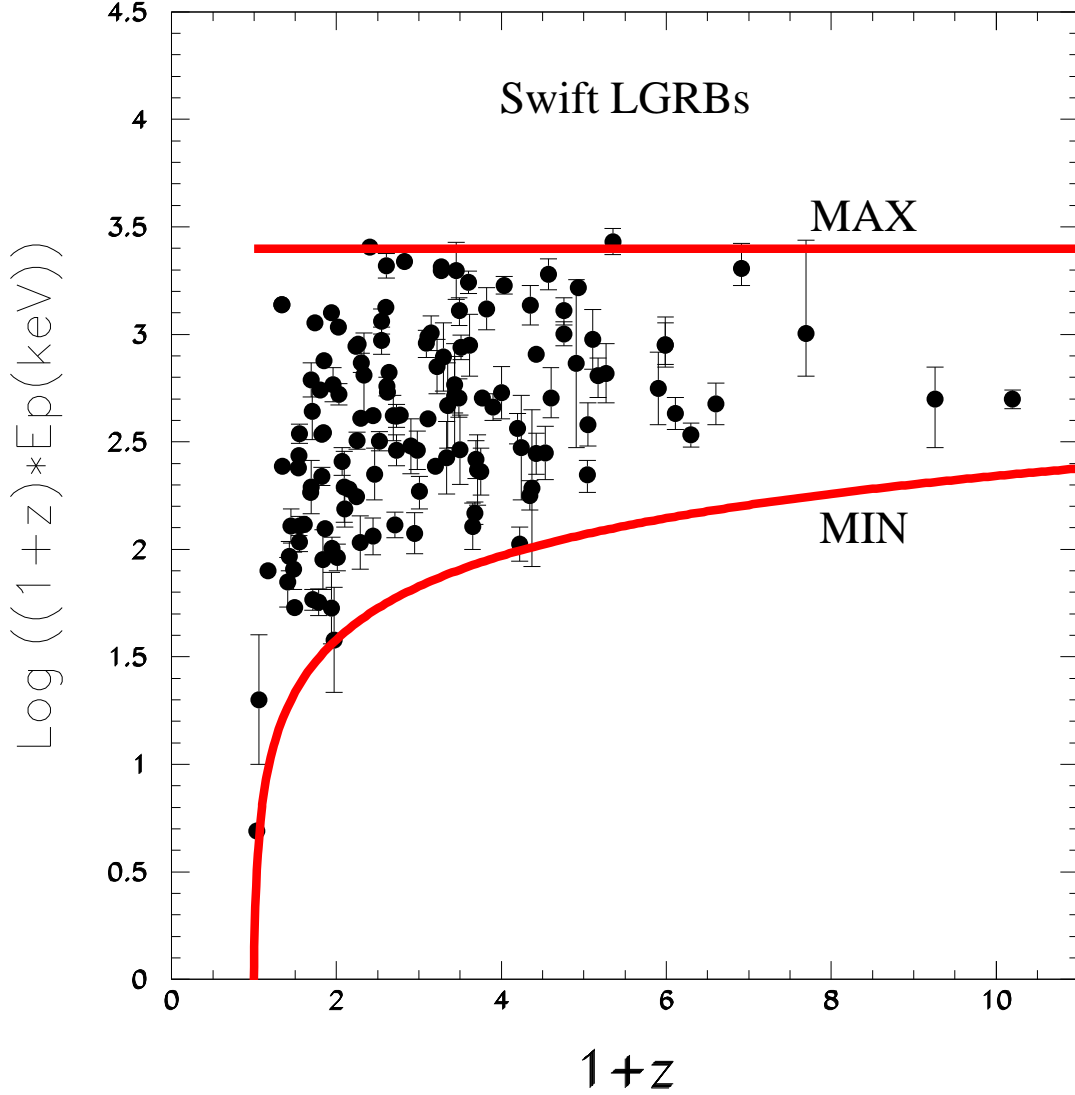


Fig. 3.— The distribution of the $E'_p(z)$ of 134 Swift LGRBs with measured redshift and E'_p , which were detected before November 15, 2013 and are listed in the Greiner catalog of GRBs. The lines represent the best fit CB model lower and upper limits, $\min E'_p(z) \propto [D_L(z)]^{1/2}$ and $\max E'_p(z) = \text{const}$, respectively, to the measured $E'_p(z)$ distribution of Swift LGRBs as function of z .

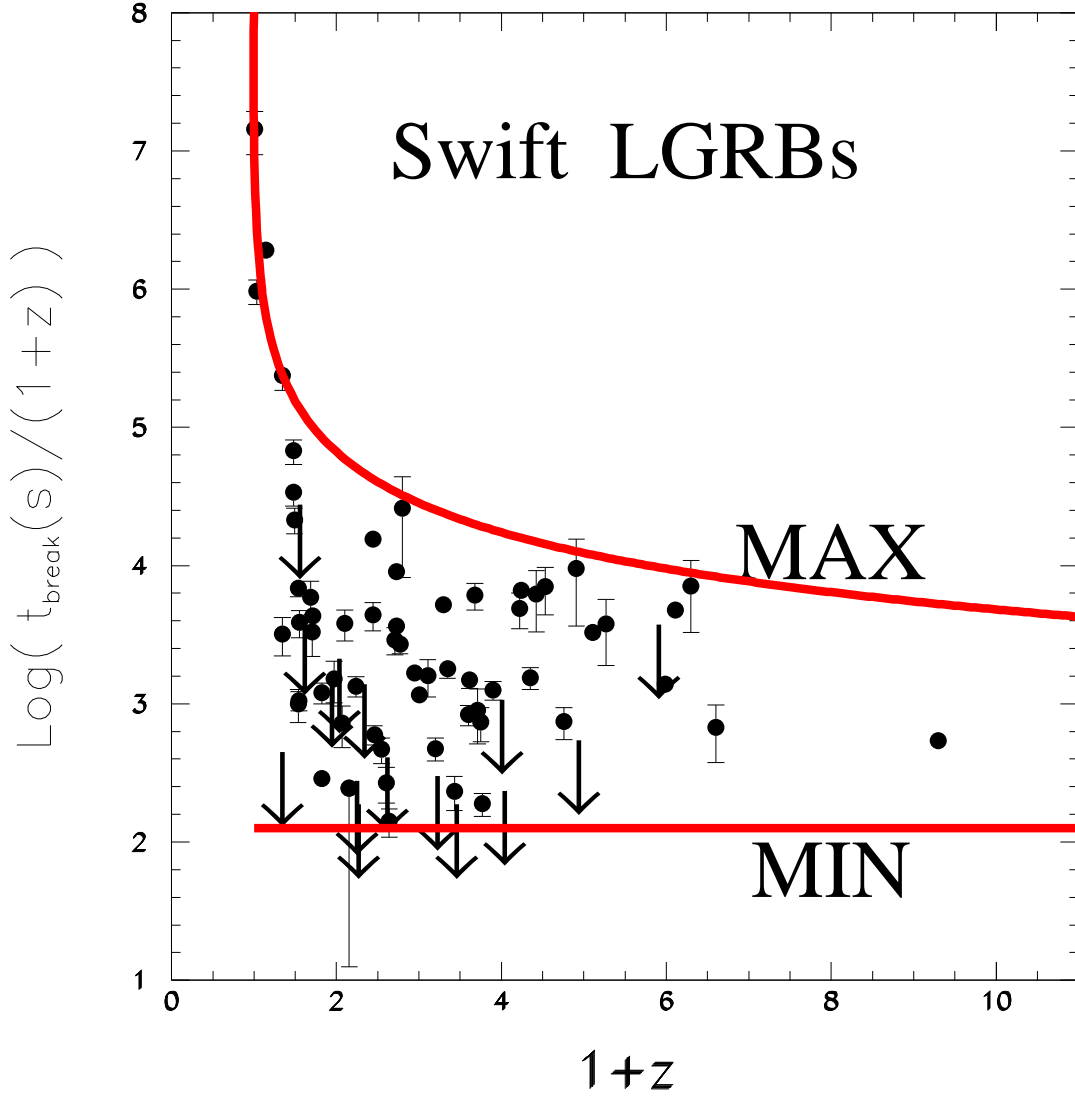


Fig. 4.— The distribution of the X-ray afterglow break time $t'_b(z)$ of 74 Swift LGRBs that were detected before November 15, 2013 and are listed in the Greiner catalog of GRBs. The lines represent lower and upper limits to the observed distribution of Swift GRBs expected in the CB model. Also shown (the highest point) is the break time of the X-ray afterglow of GRB980425 that was measured with the Chandra X-ray telescope (Kouveliotou et al. 2004)

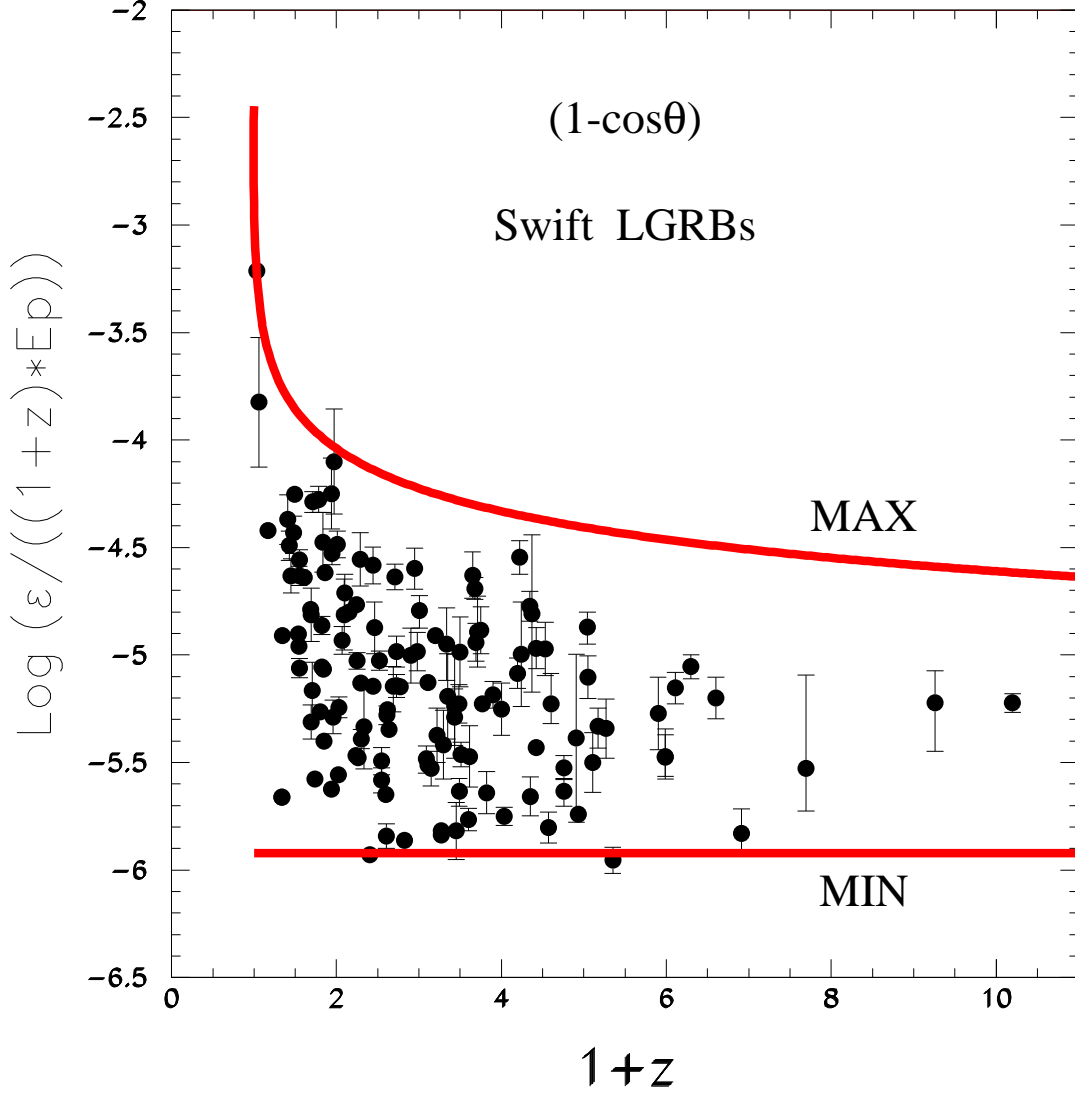


Fig. 5.— The distribution of the ratio $\epsilon_g/E'_p(z)$ for the 134 Swift LGRBs with measured redshift and E'_p , which were detected before November 15, 2013 and are listed in the Greiner catalog of GRBs. The lines represent the lower and upper limits to the distribution expected in the CB model of GRBs. The upper limit $MAX \propto [D_L(z)]^{-1/2}$ is the expected beaming factor $f_b(z)$ in the CB model.

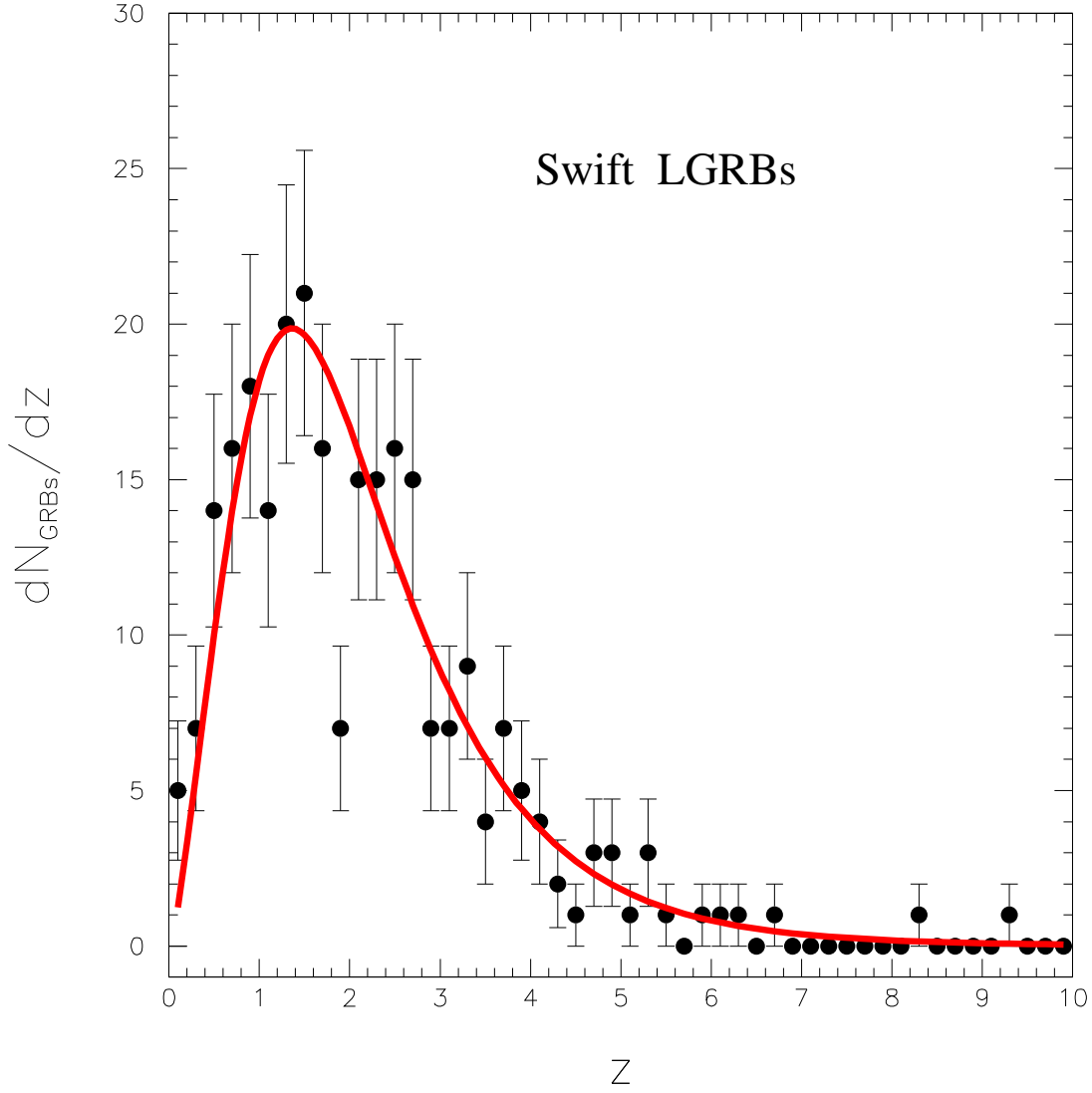


Fig. 6.— The redshift distribution of the 262 Swift LGRBs with known redshift that were detected before November 15, 2013 and the expected distribution in the CB model of LGRBs produced in SNeIc whose rate traces the SFR.

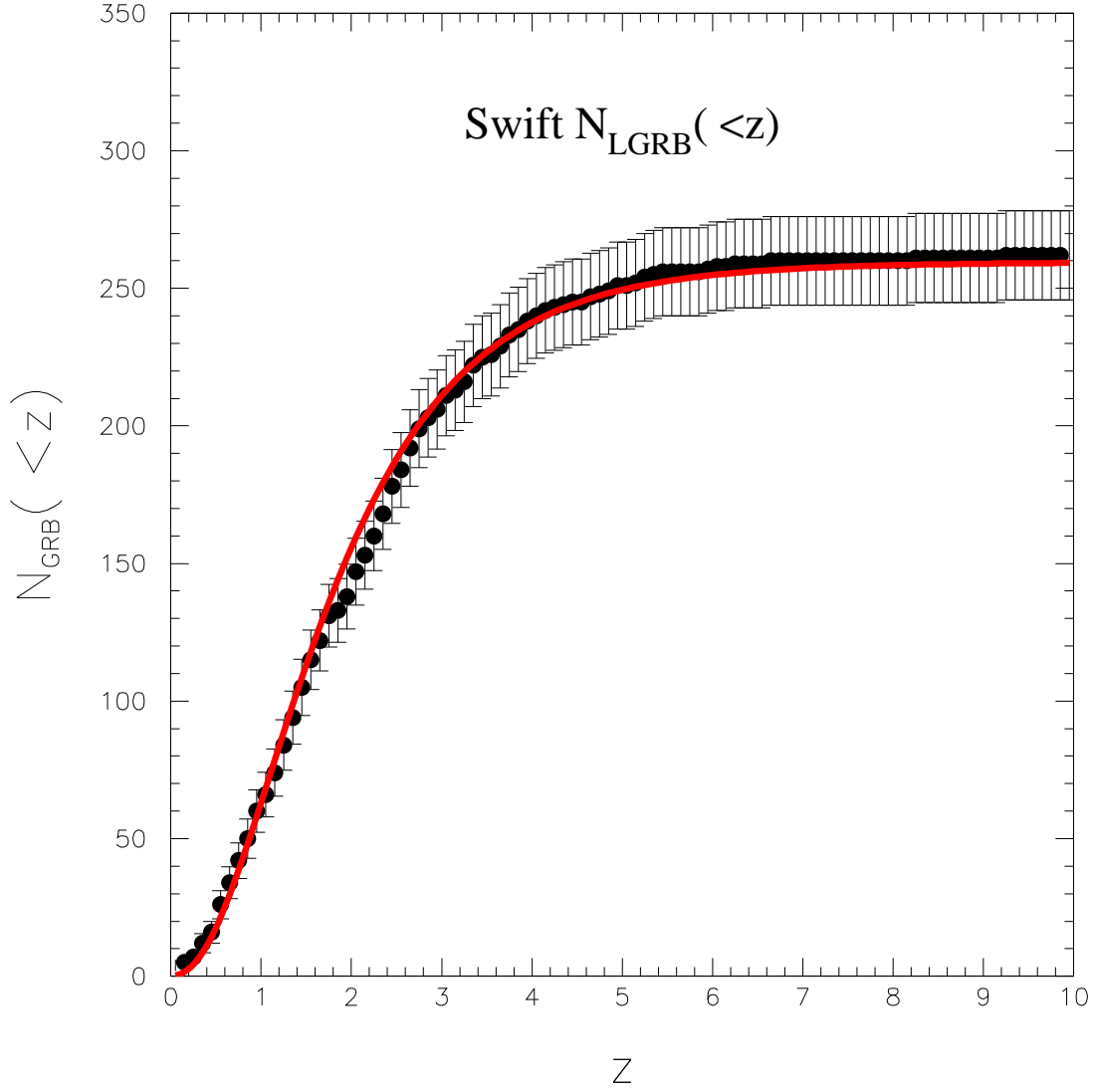


Fig. 7.— Comparison between the cumulative distribution $N(< z)$ of the 262 Swift LGRBs with known redshift that were detected before November 15, 2013 and the distribution expected in the CB model of LGRBs produced in SNeIc with a rate that traces the SFR.

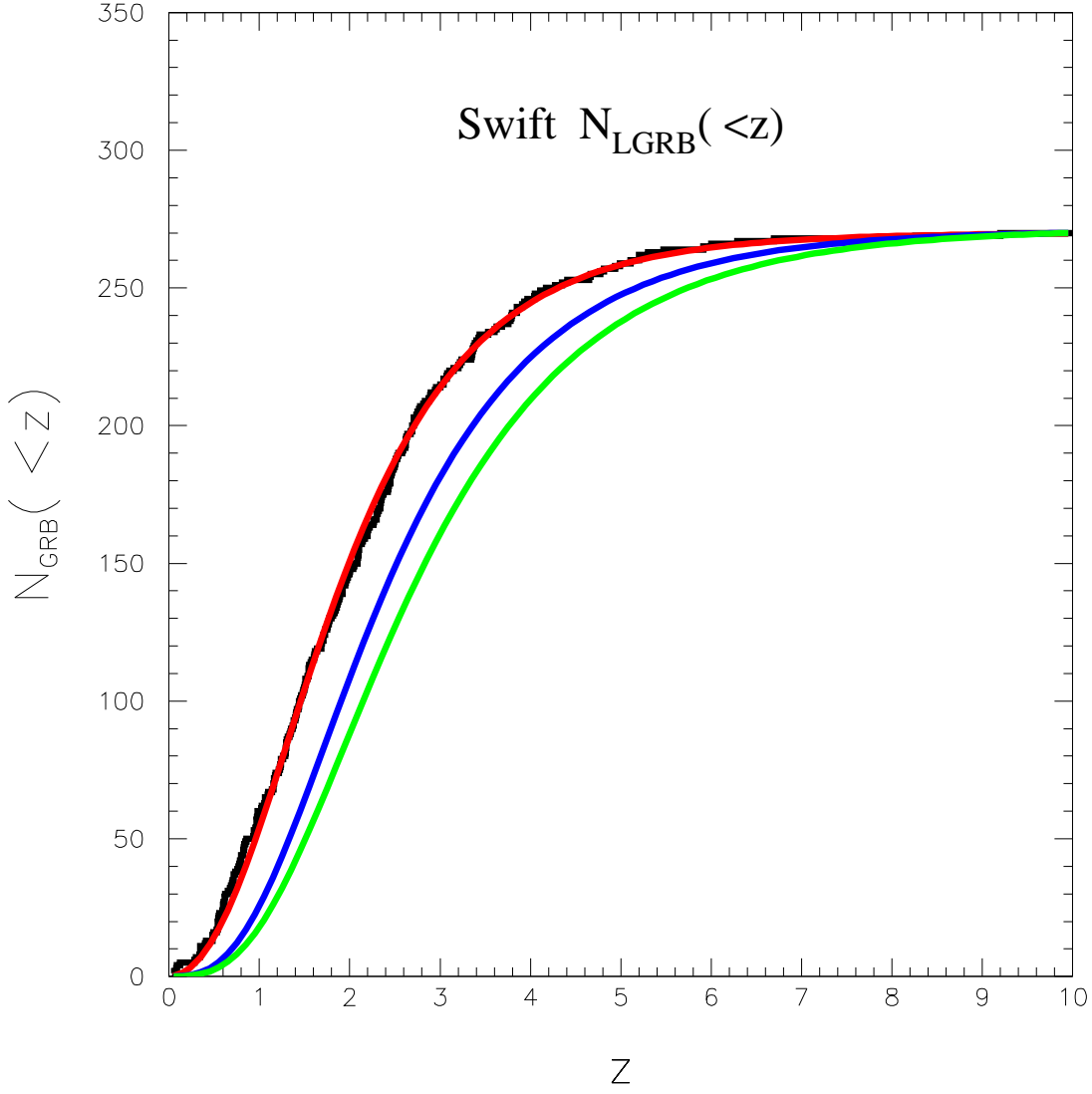


Fig. 8.— Comparison between the cumulative distribution function $N(< z)$ of the 262 LGRBs with known redshift (histogram) that were detected by Swift before November 15, 2013 after adding 8 ‘missing’ LGRBs with $1.8 \leq z \leq -2.0$, and the corresponding $N(< z)$ expected in the CB model (left curve) for LGRBs produced in SNeIc whose rate traces the SFR. Also shown are the distributions expected in the FB model with a relative evolution ($\alpha = 0.5$, right curve) and with no evolution ($\alpha = 0$, middle curve).

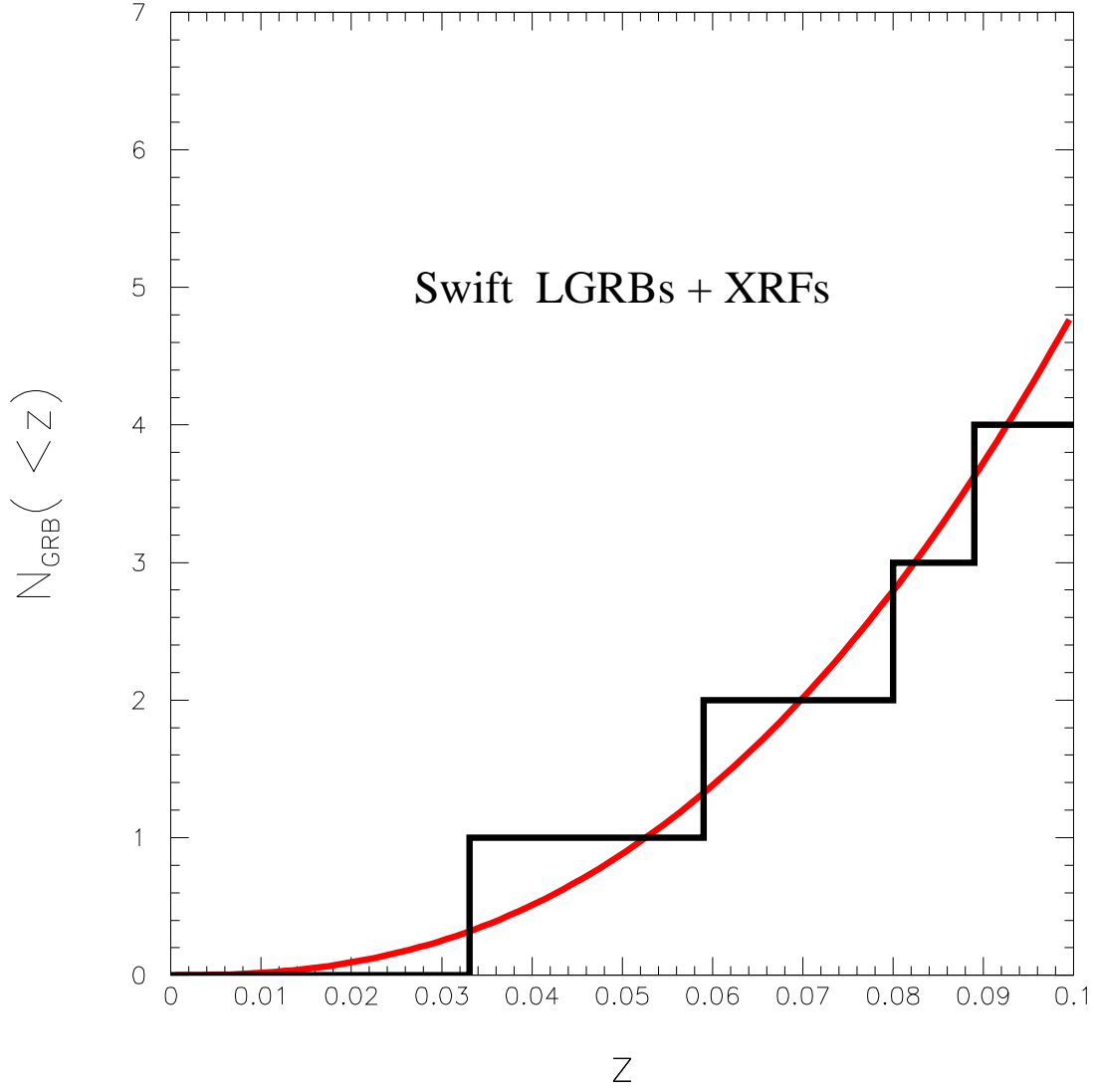


Fig. 9.— Comparison between the cumulative distribution function $N(< z)$ of LGRBs with redshift below 0.1 (hystogram) that were detected by Swift before November 15, 2013 and the CB model prediction of $N(< z)$ for $z < 0.1$ as given by Eq. (8).